http://www.aimspress.com/journal/mine

Mathematics in Engineering, 1(2): 378–390.
DOI:10.3934/mine.2019.2.378
Received: 18 January 2019
Accepted: 27 March 2019
Published: 26 April 2019

Research article

Instabilities via negative Krein signature in a weakly non-Hamiltonian DNLS model†

Panayotis G. Kevrekidis*

Department of Mathematics and Statistics, University of Massachusetts, Amherst, MA 01003-4515, USA

† **This contribution is part of the Special Issue:** Hamiltonian Lattice Dynamics
Guest Editors: Simone Paleari; Tiziano Penati
Link: http://www.aimspress.com/newsinfo/1165.html

* **Correspondence:** Email: kevrekid@math.umass.edu; Tel: +14135771977; Fax: +14135451801.

Abstract: In the present work we consider a model that has been proposed at the continuum level for self-defocusing nonlinearities in atomic Bose-Einstein condensates (BECs) in order to capture phenomenologically the loss of condensate atoms to thermal ones. We explore a model combining dispersion, nonlinearity and gain/loss at the discrete level, and illustrate the idea that modes associated with negative "energy" (mathematically: negative Krein signature) can give rise to instability of excited states when non-Hamiltonian terms are introduced in a nonlinear dynamical lattice. We showcase this idea by considering one-, two- and three-site discrete modes, exploring their stability via analytical approximations, and corroborating their continuation numerically over the relevant parameter controlling the strength of the weakly non-Hamiltonian term. We also manifest through direct numerical simulations their unstable nonlinear dynamics.

Keywords: solitary waves; instabilities; Krein signature; DNLS model

1. Introduction

One of the principal nonlinear lattice dynamical models that are used to examine the evolution of coherent structures in discrete systems is the discrete nonlinear Schrödinger equation (DNLS) [1]. One of the main reasons for its popularity is that it contains the prototypical ingredients for the manifestation of interesting phenomena, namely lattice (discrete) dispersion and nonlinearity. These features arise (in this very combination) in a wide variety of physical contexts. Most notable among them in the past two decades have, arguably, been the study of optical waveguide arrays [2–4], as well as the evolution of

atomic Bose-Einstein condensates (BECs) in the realm of optical lattice potentials [5]. These settings have, in turn, enabled not only the theoretical study, but also importantly the experimental observation of a wide array of features. Among them, a partial list includes discrete diffraction [6] and diffraction management [7], lattice solitons [6, 8, 9] and vortices [10, 11], Talbot revivals [12], and $\mathcal{PT}$-symmetry breaking [13], among many others.

On the other hand, in the context of atomic BECs, as the comprehension of their mean-field features [14, 15] is becoming more mature, it is natural to seek a deeper understanding of deviations from the standard setting, such as those involving thermal [16] and quantum [17] fluctuations. For the former, a simple phenomenological model of interest was introduced by Pitaevskii [18] and was later shown to be relevant from a microscopic perspective [19]. In fact, this so-called dissipative Gross-Pitaevskii equation (DGPE) model was also favorably compared [20], as regards nonlinear wave dynamics, with more elaborate models such as the so-called stochastic Gross-Pitaevskii equation (SGPE) model; see, e.g., [21] for a review of the latter. In addition, the DGPE model was used to predict the anti-damped motion of pairs (and triplets) of dark solitons [22] and also of multi-component solitons [23], as well as to quantify the spiraling out of the condensate of vortices [24], that was recently observed experimentally [25].

Our aim in the present work is to combine these two notions, i.e., to consider a discrete variant of the DGPE model. To simplify (technical) matters, we explore the case of the focusing nonlinearity [which corresponds to attractive interactions for a condensate inside an optical lattice], however the results can be extended to the defocusing case; see, e.g., for one such example [26]. We consider the relevant model close to the so-called anti-continuum limit, of near-vanishing coupling and explore the role of the weakly non-Hamiltonian term parameter (that we denote by γ) in the stability properties of some of the principal discrete soliton solutions. It is important to highlight that the realistic values of this parameter are quite small (e.g., the work of [24] estimates them as being between 0.00023 and 0.0023 for temperatures between 10 and 100nK in atomic BECs), nevertheless their stability impact is quite significant. The main contribution of our work is that it enables the generalization of the stability considerations (based on Lyapunov-Schmidt reductions and associated spectral calculations [27]) to this setting involving the presence of $\gamma \neq 0$. The main findings that we obtain are two-fold: On the one hand, the eigenvalues that are found to possess negative "energy" (so-called negative Krein signature, mathematically) bifurcate in *the opposite direction* than the rest of the spectrum when the weakly non-Hamiltonian perturbation is introduced. This is in line with the general theory of [28], but here the detailed calculation of these eigenvalues is provided and corroborated by our numerical findings. On the other hand, we observe that also the two-fold symmetric eigenvalue at the origin *also splits* and one of the two members of the pair moves along the real axis, leading to an instability of the most fundamental single-site soliton state. Once again, this can be attributed to the presence of the term involving γ in the model. Notice that in what follows, we will restrict considerations to the case of $\gamma > 0$, motivated by the loss of atoms for atomic BECs, although the eigenvalue expressions that we will derive will be valid irrespective of the sign of γ.

This model can be naturally placed in the context of discrete variants of the complex Ginzburg-Landau (GL) equation (for a review of its continuum form, see e.g., [29]). In what follows, we give some prototypical examples of relevant works in this GL direction from a discrete perspective and subsequently highlight the crucial elements of novelty of the present contribution. In [30], some important families of solutions in the cubic-quintic discrete GL equation were identified, including

rather exotic ones (such as cusp-like solitons) and their bifurcation diagrams were constructed. In the follow up work of [31], generalizations of on-site and inter-site solutions (with one-, and two or four-peaks, respectively) of different types were considered in the context of two spatial dimensions. More mathematically inclined works such as that of [32] were concerned with the potential convergence of the solutions of these discrete GL equations to global attractors (or their potential blowup). Another example where such models were considered was that of [33] where a discrete model bearing a saturable nonlinearity was put forth and both plane wave solutions, as well as discrete solitons and their stability were examined. It is important to highlight here that while numerous important works exist in the subject (of which the above references constitute only a representative sample), it is our understanding that there is no earlier setting putting forth an analytical evaluation of the relevant stability eigenvalues, leading to a straightforward/ easy-to-use expression such as that of Eqs. (2.12)–(2.14) below. Alongside this result, emerges an important interpretation about the expectation of stability of different modes. In particular, an explicit demonstration arises of the fact that the continuous spectrum in this case will move in a direction opposite to that of the so-called negative energy eigenvalues. To the best of our knowledge, such eigenvalue expressions, such stability intuition and its quantitative corroboration with numerical computation (in both stability and dynamics) is unprecedented in the discrete GL literature.

Our presentation of the above findings will be structured as follows. First, in section 2, we will present the model and the associated general theory for its spectral properties. Then, in section 3, we will provide existence, stability and dynamical considerations that corroborate our analytical theory for the cases of one-, two- and three-site solutions of the model. More specifically, we will examine the stability of the solutions for different values of γ. Having obtained that, we will move on to the consideration of the dynamics of the different instabilities in select case examples. We will explain how the direct dynamical results reflect the conclusions of our stability analysis. Finally, in section 4, we will summarize our findings and provide a number of directions for future study.

2. Theoretical analysis

Our starting point will be the discrete form of the DGPE as:

$$(i-\gamma)\dot{u}_n = -\epsilon\,(u_{n+1}+u_{n-1}) - |u_n|^2 u_n + \mu u_n. \tag{2.1}$$

Here, $\gamma > 0$ plays the role of the prefactor of the weakly non-Hamiltonian term, while ϵ controls the coupling between adjacent nodes of our 1d lattice. In detailed calculations that will follow including in the next section, the frequency parameter μ will be selected as $\mu = 1 + 2\epsilon$ (for convenience, given its tunability).

The steady state problem is the same in this case as it is for the standard DNLS, in particular for a given ϵ, the same stationary states that exist for $\gamma = 0$ also persist for γ finite. Hence, γ does not affect the existence properties which are well-known; see, e.g., the review in Chapter 2 of [1]. It is long established, in particular, that although at the anti-continuum (AC) [34] limit of $\epsilon = 0$, solutions of arbitrary phase $u_n = e^{i\theta_n}$ are available, for finite ϵ, the Lyapunov-Schmidt condition

$$\sin(\theta_{n+1}-\theta_n) + \sin(\theta_{n-1}-\theta_n) = 0 \tag{2.2}$$

needs to be enforced. This can be straightforwardly seen from the steady state problem of Eq. (2.1)

by multiplying with the conjugate variable $u_n^\star$. A side-by-side subtraction of the resulting algebraic equation and of its conjugate yields Eq. (2.2) upon using the AC limit expression of $u_n = e^{i\theta_n}$.

Coupled to the stipulated asymptotic decay of the solution at $n \to \pm\infty$, Eq. (2.2) leads to the phases of the solution being "locked" to $\theta_n = 0, \pi$ [27]. Solutions involving a single site (the ground state), 2-sites and 3-sites are often examined; cf., e.g., [27].

The main element where the parameter γ plays a role, however, is the stability of the solution. We now assume that the (real) solution u_n^0 is the state around which we linearize, in order to explore the spectral response of the waveform. The latter is the principal contribution of the present work in the considered discrete GL setting. Then the linearization ansatz will read:

$$u_n = u_n^0 + \delta(A_n + iB_n), \tag{2.3}$$

from which we extract the equations to $\mathrm{O}(\delta)$ for the resulting dynamical system, in order to examine the spectrum of small perturbations. We thus find:

$$\begin{pmatrix} -\gamma & -1 \\ 1 & -\gamma \end{pmatrix} \begin{pmatrix} \dot{A}_n \\ \dot{B}_n \end{pmatrix} = \begin{pmatrix} \mathcal{L}_+ & 0 \\ 0 & \mathcal{L}_- \end{pmatrix} \begin{pmatrix} A_n \\ B_n \end{pmatrix} = \mathcal{L} \begin{pmatrix} A_n \\ B_n \end{pmatrix}. \tag{2.4}$$

Here, we have defined

$$\mathcal{L}_+ = -\epsilon\Delta_2 + 1 - 3(u_n^0)^2 \tag{2.5}$$

$$\mathcal{L}_- = -\epsilon\Delta_2 + 1 - (u_n^0)^2, \tag{2.6}$$

where Δ_2 symbolizes the discrete Laplacian with unit spacing $\Delta_2 u_n = u_{n+1} + u_{n-1} - 2u_n$.

A relevant quantity to define here and in what will follow for $\epsilon \neq 0$, and $\gamma = 0$ (the Hamiltonian problem beyond the anti-continuum limit) for an eigenvalue λ_0 of the spectral problem (2.4) with the eigenvector v_0, is the Krein quantity $K(\lambda_0)$. This is defined as:

$$K(\lambda_0) := \langle \mathcal{L} v_0, v_0 \rangle, \tag{2.7}$$

where $\langle \cdot, \cdot \rangle$ is the standard inner product in l^2. The sign of this quantity, the so-called Krein signature will play a role in our considerations in what follows.

The equations resulting from Eq. (2.4), upon decomposing $A_n = a_n e^{\lambda t}$ and $B_n = b_n e^{\lambda t}$ are

$$\left(\tilde{\lambda} + \gamma\mathcal{L}_+\right) a_n = \mathcal{L}_- b_n \tag{2.8}$$

$$\left(\tilde{\lambda} + \gamma\mathcal{L}_-\right) b_n = -\mathcal{L}_+ a_n. \tag{2.9}$$

Notice also that due to the inversion of the matrix containing the γ's (and the associated determinant), in all the expressions below we rename $\lambda(\gamma^2 + 1) = \tilde{\lambda}$. In the $\gamma \to 0$ limit, $\tilde{\lambda}$ coincides with λ.

Assuming now that $\mathcal{L}_+$ is invertible, which it is close to the AC limit, where it becomes a multiplicative operator, we can write:

$$\left(\tilde{\lambda} + \gamma\mathcal{L}_+\right) \mathcal{L}_+^{-1} \left(\tilde{\lambda} + \gamma\mathcal{L}_-\right) b_n = -\mathcal{L}_- b_n \tag{2.10}$$

Now, we take advantage of the fact that near the AC limit $(u_n^0)^2 = 1$ for excited sites (given our selection of μ), hence the operator $\mathcal{L}_+$ is a multiplicative one by -2 (and thus its inverse also a multiplicative operator by $-1/2$). Then, the expression of Eq. (2.10) becomes

$$\left(\tilde{\lambda} - 2\gamma\right)\left(\tilde{\lambda} + \gamma s\right) = 2s \tag{2.11}$$

where $s = (b_n, \mathcal{L}_- b_n)$ is used to denote the small eigenvalues of the operator $\mathcal{L}_-$ that have been previously computed explicitly in the Hamiltonian limit; see e.g., [27]. This then leads to the principal result of the present work, namely that the model with $\gamma \neq 0$ will possess eigenvalues of the form:

$$\tilde{\lambda} = \frac{\gamma(2-s) \pm \sqrt{\gamma^2(s-2)^2 + 8s(\gamma^2+1)}}{2}. \tag{2.12}$$

We will bear in mind in what follows (also, per the motivating example mentioned in the Introduction) that practically $\gamma^2 \ll 1$. We now consider some special cases. We first mention the one in the immediate vicinity of the AC limit, whereby $s = \mathrm{O}(\epsilon) \ll 1$. Then,

$$\tilde{\lambda} = \gamma \pm \sqrt{\gamma^2 + 2s}. \tag{2.13}$$

I.e., for the eigenvalues that bifurcate from 0, of which, as the theory of [27] suggests, there are at least $N-1$ pairs in the Hamiltonian case (we will treat the eigenvalue pair at 0 separately below), we find that they will *generically* lead to instability; N here denotes the number of excited nodes/sites of the lattice. This is because if $s > 0$ (i.e., for eigenvalues leading to real instabilities even in the Hamiltonian case), at least one of them will be real and positive even in the presence of the terms involving γ, per Eq. (2.13). On the other hand, if $s < 0$, as occurs for the eigenvalues of negative energy in the Hamiltonian case of [27], we have the following. For sufficiently small γ, i.e., $\gamma < \sqrt{2|s|}$, the relevant imaginary (for the Hamiltonian case) eigenvalues will turn complex with a positive real part. Eventually, these eigenvalues will collide on the positive real axis at $\gamma = \sqrt{2|s|}$, splitting off as real thereafter. It is particularly relevant to point out that *all* the rest of the eigenvalues move to the left half spectral plane (stable eigendirections), reflecting the lossiness present in the problem. Nevertheless, the eigenvalues that emerged from the origin in the Hamiltonian case of [27], because of their negative Krein signature (the sign of the quantity defined in Eq. (2.7)) move in the *opposite* direction, as our main result clearly indicates and give rise to pairs of complex eigenvalues. If there are $N-1$ such eigenvalues with $s < 0$ for an N-site configuration (as is the case when adjacent excited sites have alternating phases), then there are going to be $N-1$ complex pairs of associated eigenvalues emerging for $\gamma > 0$.

A special mention deserves to be made for the limit of $s = 0$. It turns out that the above formulae yield the correct result for the asymptotic case with $s = 0$. There exists, as is well-known [1], a pair of eigenvalues at the origin, due to the phase invariance in the Hamiltonian case of $\gamma = 0$. The solution itself remains an eigenvector with vanishing eigenvalue in this case, however the presence of $\gamma \neq 0$ avoids the persistence of the generalized corresponding eigenmode. It is for that reason that the eigenvalues (of this pair) in this context split when $\gamma \neq 0$, becoming $\tilde{\lambda} = 2\gamma$ and 0, according to Eq. (2.13). We will see indeed that the relevant expression provides a very good approximation to the corresponding unstable mode in what follows.

Lastly, it is important to point out that it is possible to follow the same type of analysis for the continuous spectrum eigenmodes, taking into consideration the facts that:

(a) the relevant eigenvalues can be identified via linearization around the vanishing state with $u_n^0 = 0$;

(b) in this limit $\mathcal{L}_+ = \mathcal{L}_-$.

Then, the relevant calculation stemming from Eq. (2.10) for plane waves $\propto e^{i(kn-\omega t)}$ is considerably simplified and gives rise to a continuous spectrum explicitly calculable as:

$$\tilde{\lambda} = \left(1 + 4\epsilon \sin^2(\frac{k}{2})\right)(-\gamma \pm i). \tag{2.14}$$

It is straightforward to see that the introduction of the parameter γ sends the continuous spectrum to the left half plane, contrary -as we saw above- to what is the case for the eigenvalues of negative signature.

3. Numerical computations

We now explore a diverse array of states that are well-known to exist in the DNLS model, since the steady state problem herein, being the same as in the case of DNLS still gives rise to such states. In what follows, we will set $\epsilon = 0.01$ in the vicinity of the AC limit and will vary γ as a parameter of the model.

We start from the single-site configuration of Figure 1. The left panel of the figure illustrates the exponential decay of the spatial profile of the configuration. The spectrum of this mode for $\gamma = 0$ (the ground state of the Hamiltonian problem) features a pair of eigenvalues at the origin, as well as a continuous spectrum extending across the interval $\pm i(1+4\epsilon \sin^2(k/2))$. As soon as $\gamma > 0$ is introduced, the latter modes, move to the left half plane as is illustrated in the bottom panel of Figure 1. On the other hand, in line with the predictions of Eqs. (2.12) and (2.13), the pair of modes at 0 splits; one of them remains at the origin, due to the phase invariance, while the other moves along the real line with $\lambda = 2\gamma/(\gamma^2+1)$ and gives rise to the instability of the solution. The comparison of the theoretical prediction with the numerical result is excellent (for this eigenmode, as well as for the entire spectrum) and is shown in the right panel of Figure 1.

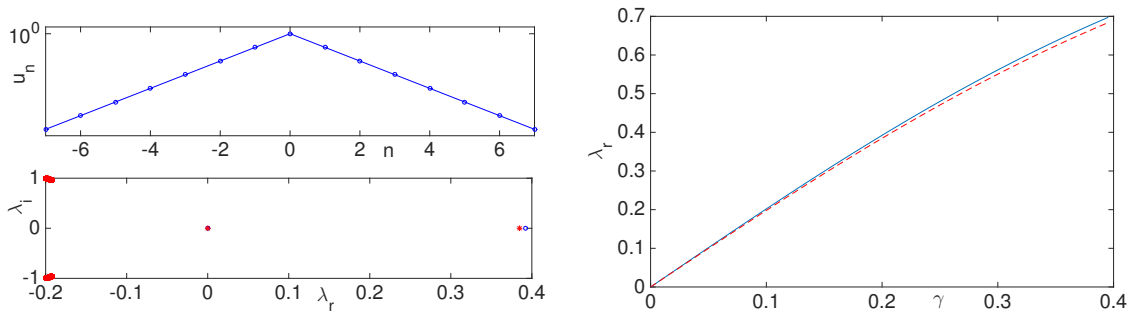

Figure 1. The left panel illustrates the spatial profile in a semi-log plot, indicating the exponential decay, as well as the corresponding spectral plane for $\gamma = 0.2$. In the latter, both the numerically identified spectral modes $\lambda = \lambda_r + i\lambda_i$ are given (as blue circles) and the theoretical predictions stemming from application of Eq. (2.10) for the different modes are provided (as red stars) for comparison. The right panel shows the unstable mode exiting as real from $(0,0)$ (solid blue line) and its corresponding theoretical prediction $(2\gamma/(\gamma^2+1)$ as red dashed line). Here $\epsilon = 0.01$ is chosen.

The next case that we consider is that of the so-called anti-symmetric or twisted localized modes [35]. Such modes are well-known to be stable in the Hamiltonian case of $\gamma = 0$ near the AC limit, due to a pair at the origin (phase invariance) and another pair $\lambda = \pm 2\sqrt{\epsilon} i$, associated with $s = -2\epsilon$ [27]. This gives an immediate prediction that can be used, in addition to the predictions that we had before for the mode emerging from $(0,0)$ and the continuous spectrum in the spectral plane (λ_r, λ_i) of eigenvalues $\lambda = \lambda_r + i\lambda_i$. In this case, in the left panel of the figure we show two distinct

cases, namely $\gamma = 0.1$ and 0.3. This is because the two of them are separated by the critical point $\gamma = \sqrt{2|s|}$ of Eq. (2.13). As predicted in our theory of the previous section, the modes become immediately unstable (for $\gamma > 0$), giving rise to a complex pair. Eventually, however, the two eigenvalues of the pair collide at $\gamma = \sqrt{2|s|} = 2\sqrt{\epsilon}$ (= 0.2 in this case) and subsequently exit along the real axis. We find this feature to be in excellent agreement once again with the numerical findings both as regards the general phenomenology, but also as regards the quantitative aspects (critical point, etc.).

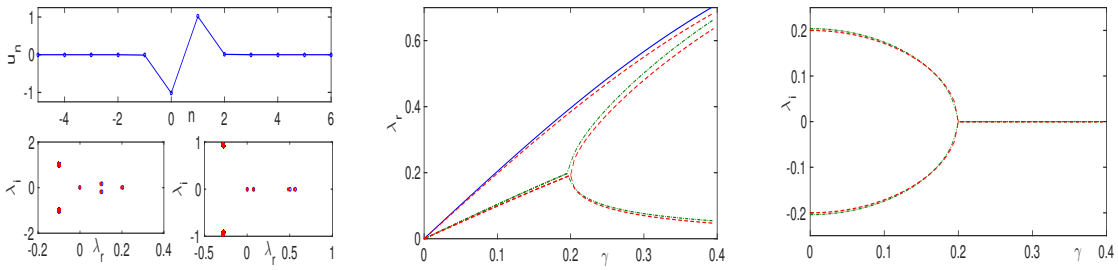

Figure 2. The figure considers the case of the two-site, out-of-phase mode (sometimes referred to as "twisted" localized mode [35]). The left panel illustrates once again the stationary state, while its corresponding spectrum is shown for $\gamma = 0.1$ and 0.3 (in excellent comparison between the blue circles of the numerics and the red stars of the theory). The middle and right panels illustrate the dominant (unstable) eigenmodes and how they move: one of them, as before and using also the same symbolism, emerges from $(0, 0)$. However, importantly, two more become immediately complex (see the green dash-dotted lines), in excellent agreement with the theoretical prediction (red dashed lines) and eventually collide near $\gamma = 2\sqrt{\epsilon} = 0.2$ (here $\epsilon = 0.01$), giving rise to a real pair thereafter.

We now turn to the case of the two-site in-phase configuration. This is a state that is well-known in the Hamiltonian limit to be unstable for all values of the coupling ϵ, due to a real pair $\lambda = \pm\sqrt{2s} = \pm 2\sqrt{\epsilon}$. For $\gamma > 0$, using $s = 2\epsilon$, we find that one of the members of the real pair (the positive one) grows rapidly in excellent agreement with the predictions of Eqs. (2.12) and (2.13), while the negative counterpart tends to 0. Additionally, the mode from $(0, 0)$ is still present (although now the instability is dominated by the already real mode at $\gamma = 0$). Finally, the continuous spectrum moves again to the left half plane. All the modes are captured very accurately by the theoretical analysis.

Lastly, to illustrate that the relevant phenomenology can, in principle, be applied to *arbitrary* configurations, we consider a three-site solution. As is well-known, once again from the Hamiltonian limit, the only one among them that can be stable for finite values of $\epsilon \neq 0$, is the twisted mode involving three excited sites and two sign changes between them i.e., $(+, -, +)$ or $(-, +, -)$ if we consider a symbolic representation of the signs of the relevant solution's excited sites. This configuration is shown in the left panel of Figure 4, along with the corresponding spectral planes for both $\gamma = 0.1$ and $\gamma = 0.3$. As the middle panel involving the real parts and the right panel involving the imaginary ones illustrate, for this solution, there are two modes that become complex; once again these stem from the two negative Krein signature modes that are known to exist in the Hamiltonian limit of $\gamma = 0$ [27]. For these modes, the Hamiltonian limit yields $s = -\epsilon$ and $s = -3\epsilon$, which implies that they will respectively be complex—in line with the approximate Eq. (2.13)—until

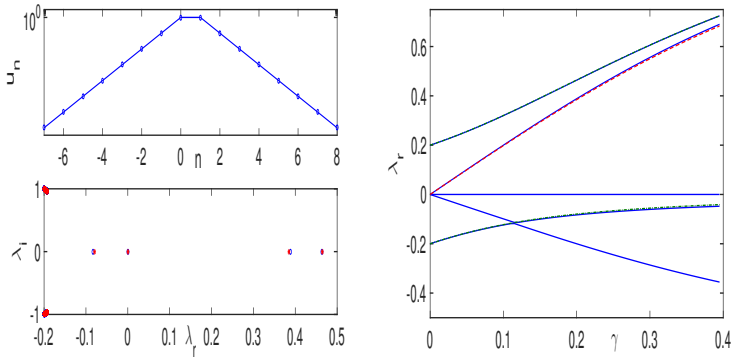

Figure 3. This figure concerns the in-phase mode with two excited sites. The mode also decays exponentially and is unstable already from the limit of $\gamma = 0$ and onwards. The spectral plane of the case with $\gamma = 0.2$ showcases the excellent agreement with the theoretical results. The right panel yields all the numerical modes (the unstable pair of $\gamma = 0$ –starting at ± 0.2 and growing–, the eigenvalue growing from the origin, and the continuous spectrum moving to the left i.e., downward in the panel) in solid blue line. The red-dashed is the theory for the mode emerging from $(0, 0)$, and the green dash-dotted curves that can barely be distinguished from the blue solid ones showcase the excellent agreement of the modes predicted by Eqs. (2.12) and (2.13) for $s = 2\epsilon$. Recall that here $\epsilon = 0.01$.

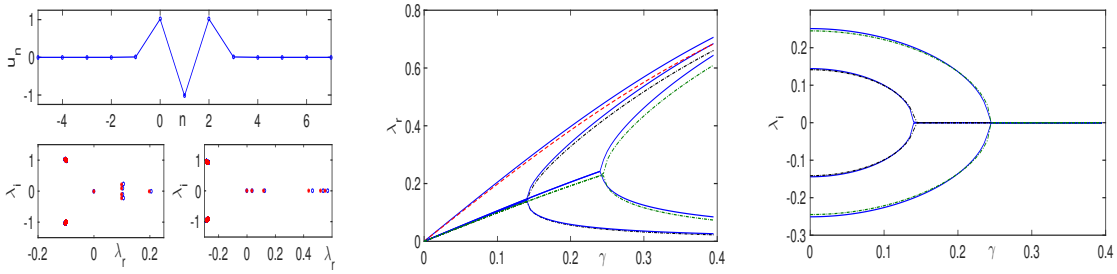

Figure 4. Similar to the previous cases (most notably Figure 2) but now for the twisted three-site configuration of opposite adjacent signs, i.e., $(+, -, +)$. The left panel shows the solution profile and its spectral planes for $\gamma = 0.1$ (with two complex pairs and a real one, as well as the continuous spectrum) and for $\gamma = 0.3$, past the two critical points, where the two complex pairs have collided on the real axis becoming real. The configuration, in addition to the (most) unstable mode stemming from $\lambda = 0$, features the two complex –at least for small γ– pairs; their theoretical prediction is shown in green and black dash-dotted lines in the middle and right panel, respectively, for the real and imaginary parts. These compare very well with the corresponding numerical ones in blue solid lines. Here $\epsilon = 0.01$.

$\gamma_{cr}^{(1)} = \sqrt{2\epsilon} \approx 0.1414$ and $\gamma_{cr}^{(2)} = \sqrt{6\epsilon} \approx 0.245$. The middle and right panels of Figure 4 indicate that these critical points, but also the overall behavior of the relevant eigenvalues is in very good agreement with the numerical observations. Indeed, prior to the critical points, the respective pairs are complex, subsequently splitting along the real axis with two of the four eigenvalues growing and two shrinking towards 0. In addition to these modes, there is the single eigenvalue $2\gamma/(\gamma^2 + 1)$, growing from the origin, which in fact turns out to be the most unstable mode of the system.

We now complement these results with some direct numerical simulations, to showcase how these findings manifest themselves therein. We start from a simulation of the single-site solution illustrated in Figure 5. There, we can see that indeed in this case, as expected from the theory, exponential growth manifests itself. This is shown by comparing the evolution of a slightly perturbed central site $|u_0|^2$ with the corresponding steady state value $|u_0^s|^2$ and seeing how the difference starting from around 10^{-4} grows in an exponential fashion (blue solid line), linear in the semilog plot, matching very closely the theoretical dashed red line, pertaining to the growth rate of the mode emerging from $(0, 0)$ in the spectral plane [recall that its growth rate is given by $2\gamma/(\gamma^2 + 1)$].

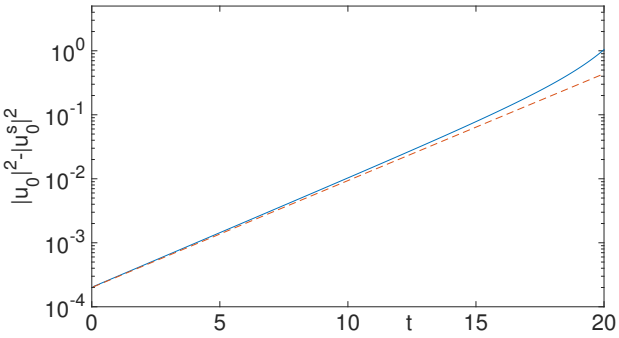

Figure 5. For a small initial perturbation to the single site solution, we explore how its central site $|u_0|^2$ grows in comparison to the steady state value $|u_0^s|^2$. The solid blue line corresponds to the numerical computation while the dashed red line to the theoretical prediction for this growth. The coupling is given by $\epsilon = 0.01$.

We next consider the case example of the twisted mode for the two cases that were already shown in Figure 2, namely $\gamma = 0.1$ and $\gamma = 0.3$. Figure 6 illustrates that in the former case, a fundamentally distinct feature emerges, namely the emergence of oscillatory growth. This is natural to expect given the presence of complex eigenvalues in the system. However, given that they do not constitute the dominant mode and the growth is fairly rapid, we have suitably zoomed in to observe how the dynamics concurrently features oscillations and growth in the early stages of the manifestation of the instability. This is to be contrasted with the case of the right panel for $\gamma = 0.3$, where the theory predicts purely real eigenvalues (due to the complex pairs' collision) and purely exponential growth. Indeed, in the case shown one of the sites grows while the other one decays.

As a final example [*], we consider the example of the two-site solution where the excited sites are in-phase. Figure 7 captures the relevant phenomenology illustrating the growth of one of the two sites

[*]For the case of three sites, we generally observed similar features to the ones above, with oscillatory growth dynamics for small enough γ and exponential growth for sufficiently large γ hence we do not lend separate consideration to that case here.

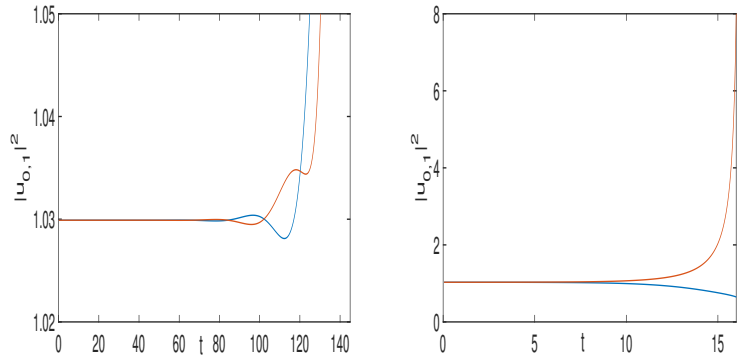

Figure 6. Evolution of the two central sites of the solution with $n = 0$ and $n = 1$ in the case of a two-site (twisted mode) solution. The left panel featuring oscillatory growth away from the steady state is shown for the case of $\gamma = 0.1$ (where a complex pair exists in the linearization), while the right panel featuring exponential deviation from the stationary state is for the case of $\gamma = 0.3$. As before, the parameter ϵ is set to $\epsilon = 0.01$.

of the solution. It can be seen again that the early stages of the growth are captured by the relevant mode of the linearization (cf. the most dominant mode, the one starting as real already for $\gamma = 0$ in the case of Figure 3). It is worth noting, however, that although the 2nd (and neighboring) node also features growth at the early stages, eventually the solution's amplitude symmetry is broken and one of the two nodes (here the $n = 0$ node) grows faster than the other one.

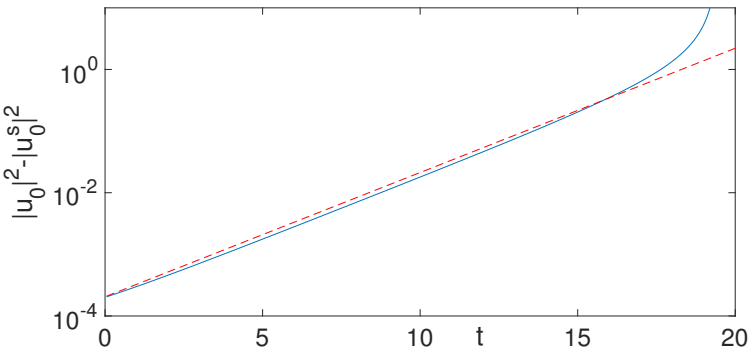

Figure 7. Evolution of the $n = 0$ node in a two-site in-phase solution numerically (blue solid line) vs. the theory of the most unstable mode for $\gamma = 0.2$ in Figure 3. Good agreement is again found between the theoretical result and the numerical observation. Again, we have set $\epsilon = 0.01$.

4. Conclusions & future challenges

In the present work, we have revisited the widely relevant DNLS model in the context of a phenomenological non-conservative term introduced originally for finite temperature atomic condensates. This gave us the opportunity to examine the spectral properties of solitary wave

solutions of the model in the presence of weakly non-Hamiltonian perturbations. The relevant setting induces a lossy effect at the linear level, which is responsible for the motion to the left of the continuous spectrum, however, there is concurrently a gain effect at the nonlinear level due to the self-focusing nonlinearity. This introduces an interesting competition in the model. What we were able to analytically illustrate in the present setting is that the eigenvalues bifurcating from the origin (and associated with the nonlinear states of the model) move in the *opposite direction* than the rest of the spectrum and towards the right half of the spectral plane, giving rise to instabilities. One such mode comes from the origin (and is *generically* present), while additional ones stem either from real modes (when present) and asymmetrize them, or from imaginary ones (when present), rendering the latter complex, until they collide on the real axis, at a finite predictable value of the parameter γ. Remarkably, we saw that the direct analysis of this non-Hamiltonian model eigenvalue problem, combined with a detailed understanding of the Hamiltonian version of the relevant operators (borrowed from [27]) provides a complete and highly accurate spectral picture for this system. Lastly, it should be pointed out that the relevant features (instabilities, via oscillatorily or exponentially growing modes) have also been corroborated via direct numerical simulations.

It would be interesting to extend the present considerations to different classes of systems. One can consider other forms involving gain and loss in NLS (see, e.g., for a relevant recent example [36]), hence it would be relevant to explore to what degree the considerations herein would apply there. In particular, the analysis presented here does not address the general dissipative case; it is more restricted to (weak) perturbations of the Hamiltonian problem that destroy its Hamiltonian nature. Nevertheless, we expect that some of these properties (e.g., the motion of eigenvalues of negative Krein signature under weakly non-Hamiltonian perturbations) should be of broader relevance than the specific context considered herein. However, exploring the extent to which these topological considerations apply and where they may fail will be of particular interest for future studies. It would also be of interest to explore this, as well as other models in higher dimensional settings to examine their implications on both soliton and the more elaborate vortex solutions featured in the latter [1]. Such studies will be considered in future publications.

Acknowledgements

This material is based upon work supported by the U.S. National Science Foundation under Grant No. PHY-1602994 and under Grant No. DMS-1809074. The author also acknowledges the support by NPRP GRant [9-329-1-067] from Qatar National Research Fund (a member of Qatar Foundation). The findings achieved herein are solely the responsibility of the author.

Conflict of interest

The author declares no conflict of interest.

References

1. Kevrekidis PG (2009) *The Discrete Nonlinear Schrödinger Equation: Mathematical Analysis, Numerical Computation and Physical Perspectives*, Heidelberg: Springer-Verlag.

2. Christodoulides DN, Lederer F, Silberberg Y, Christodoulides DN (2003) Discretizing light behavior in linear and nonlinear waveguide lattices. *Nature* 424: 817–823.
3. Sukhorukov AA, Kivshar YS, Eisenberg HS, et al. (2003) Spatial optical solitons in waveguide arrays. *IEEE J Quantum Elect* 39: 31–50.
4. Lederer F, Stegeman GI, Christodoulides DN, et al. (2008) Discrete solitons in optics. *Phys Rep* 463: 1–126.
5. Morsch O, Oberthaler M (2006) Dynamics of Bose-Einstein condensates in optical lattices. *Rev Mod Phys* 78: 179–215.
6. Eisenberg HS, Silberberg Y, Morandotti R, et al. (1998) Discrete spatial optical solitons in waveguide arrays. *Phys Rev Lett* 81: 3383–3386.
7. Eisenberg HS, Silberberg Y, Morandotti R, et al. (2000) Diffraction management. *Phys Rev Lett* 85: 1863–1866.
8. Morandotti R, Peschel U, Aitchison JS, et al. (1999) Dynamics of discrete solitons in optical waveguide arrays. *Phys Rev Lett* 83: 2726–2729.
9. Morandotti R, Eisenberg HS, Silberberg Y, et al. (2001) Self-focusing and defocusing in waveguide arrays. *Phys Rev Lett* 86: 3296–3299.
10. Neshev DN, Alexander TJ, Ostrovskaya EA, et al. (2004) Observation of discrete vortex solitons in optical induced photonic lattices. *Phys Rev Lett* 92: 123903.
11. Fleischer JW, Bartal G, Cohen O, et al. (2004) Observation of vortex-ring "discrete" solitons in 2D photonic lattices. *Phys Rev Lett* 92: 123904.
12. Iwanow R, May-Arrioja DA, Christodoulides DN, et al. (2005) Discrete Talbot effect in waveguide arrays. *Phys Rev Lett* 95: 053902.
13. Rüter CE, Makris KG, El-Ganainy R, et al. (2010) Observation of parity-time symmetry in optics. *Nat Phys* 6: 192–195.
14. Pitaevskii LP, Stringari S (2003) *Bose-Einstein Condensation*, Oxford: Oxford University Press.
15. Kevrekidis PG, Frantzeskakis DJ, Carretero-González R (2015) *The Defocusing Nonlinear Schrödinger Equation*, Philadelphia: SIAM.
16. Proukakis N, Gardiner S, Davis M, et al. (2013) *Quantum gases: Finite Temperature and Nonequilibrium Dynamics*, London: Imperial College Press.
17. Carr LD (2010) *Understanding Quantum Phase Transitions*, Boca Raton: CRC Press Taylor & Francis Group.
18. Pitaevskii LP (1959) Phenomenological theory of superfluidity near the λ point. *Sov Phys JETP* 35: 282–287.
19. Jackson B, Proukakis NP (2008) Finite temperature models of Bose-Einstein condensation. *J Phys B: At Mol Opt Phys* 41: 203002.
20. Cockburn SP, Nistazakis HE, Horikis TP, et al. (2010) Matter wave dark solitons: Stochastic versus analytical results. *Phys Rev Lett* 104: 174101.
21. Cockburn SP, Proukakis NP (2009) The stochastic Gross-Pitaevskii and some applications. *Laser Phys* 19: 558–570.

22. Kevrekidis PG, Frantzeskakis DJ (2011) Multiple dark solitons in Bose-Einstein condensates at finite temperatures. *Discrete Contin Dyn Sys* 4: 1199–1212.
23. Achilleos V, Yan D, Kevrekidis PG, et al. (2012) Dark-bright solitons in Bose-Einstein condensates at finite temperatures. *New J Phys* 14: 055006.
24. Yan D, Carretero-González R, Frantzeskakis DJ, et al. (2014) Exploring vortex dynamics in the presence of dissipation: analytical and numerical results. *Phys Rev A* 89: 043613.
25. Moon G, Kwon WJ, Lee H, et al. (2015) Thermal friction on quantum vortices in a Bose-Einstein condensate. *Phys Rev A* 92: 051601.
26. Kevrekidis PG, Susanto H, Chen Z (2006) Higher-order-mode soliton structures in two-dimensional lattices with defocusing nonlinearity. *Phys Rev E* 74: 066606.
27. Pelinovsky DE, Kevrekidis PG, Frantzeskakis DJ (2005) Stability of discrete solitons in nonlinear Schrödinger lattices. *Phys D* 212: 1–19.
28. Kapitula T, Kevrekidis PG, Sandstede B (2004) Counting eigenvalues via the Krein signature in infinite-dimensional Hamiltonian systems. *Phys D* 195: 263–282.
29. Aranson IS, Kramer L (2002) The world of the complex Ginzburg-Landau equation. *Rev Mod Phys* 74: 99–143.
30. Efremidis NK, Christodoulides DN (2003) Discrete Ginzburg-Landau solitons. *Phys Rev E* 67: 026606.
31. Efremidis NK, Christodoulides DN, Hizanidis K (2007) Two-dimensional discrete Ginzburg-Landau solitons. *Phys Rev A* 76: 043839.
32. Karachalios NI, Nistazakis HE, Yannacopoulos AN (2007)Asymptotic behavior of solutions of complex discrete evolution equations: the discrete Ginzburg-Landau equation. *Discrete Contin Dyn Sys-Ser A* 19: 711–736.
33. Kiselev Al S, Kiselev An S, Rozanov NN (2008) Dissipative discrete spatial optical solitons in a system of coupled optical fibers with the Kerr and resonance nonlinearities. *Opt Spectrosc* 105: 547–556.
34. MacKay RS, Aubry S (1994) Proof of existence of breathers for time-reversible or Hamiltonian networks of weakly coupled oscillators. *Nonlinearity* 7: 1623–1643.
35. Darmanyan S, Kobyakov A, Lederer F, et al. (1998) Stability of strongly localized excitations in discrete media with cubic nonlinearity. *J Exp Theor Phys* 86: 682–686.
36. Achilleos V, Bishop AR, Diamantidis S, et al. (2016) Dynamical playground of a higher-order cubic Ginzburg-Landau equation: From orbital connections and limit cycles to invariant tori and the onset of chaos. *Phys Rev E* 94: 012210.

AIMS Press